

<https://doi.org/10.37434/tpwj2022.04.04>

FIBRE LASER WELDING OF ALUMINIUM ALLOYS OF 7xxx SERIES (Al–Zn–Mg–Cu) BY NONTHROUGH THICKNESS WELDS

V.M. Korzhyk^{1,2}, V.Yu. Khaskin^{1,2}, A.A. Grynyuk², S.I. Peleshenko³, Yao Yuhui⁴,
S.G. Hrygorenko², V.O. Shcheretskyi², O.S. Kushnareva²

¹China-Ukraine E.O. Paton Institute of Welding of Guangdong Academy of Sciences.
Guandong Provincial Key Laboratory of Advanced Welding Technology
Guangzhou, 510650, China

²E.O. Paton Electric Welding Institute of the NASU
11 Kazymyr Malevych Str., 03150, Kyiv, Ukraine

³National Technical University of Ukraine «Igor Sikorsky Kyiv Polytechnic Institute»
37 Peremohy Ave., 03056, Kyiv, Ukraine

⁴Shenzhen Hanzhizi Technology Co., Ltd.

6th Floor. Building B, Bantian International Center, 5 Huancheng South Road, Longgang District,
Shenzhen, Guangdong, China

ABSTRACT

The paper deals with the features of laser welding with incomplete (nonthrough thickness) penetration of high-strength aluminium alloys of 7xxx series. It was found that at joining of 1.5 mm sheets by fibre laser welding to the depth of 0.5–0.7 mm there arises the risk of formation of pores, in particular, in the root zone, streaks of oxide film in the weld lower part, as well as hot cracks. The latter can be eliminated by reducing the welding heat input below 25–30 J/mm. The weld metal is characterized by an equiaxed finely dispersed structure with grain size of 10–15 μm for 7005 alloy and 15–25 μm for 7075 alloy. In the fusion zone, the grains are of an elongated shape with 2.5–3.0 coefficient for 7005 alloy and 2–5 for 7075 alloy. In the HAZ the grain length is reduced, the shape coefficient becomes 3–5 and 3.0–3.5 for 7005 and 7075 alloys, respectively. At performance of laser welding with small (~5 J/mm) values of the heat input, microhardness of the welds and HAZ is rather uniform, and close to that of the base metal. For 7075 alloy microhardness drop to 20 % was observed in the fusion zone region that is due to formation of grains of an elongated shape with shape coefficient of 2–5. The found drawbacks can be eliminated through reduction of pulsations of the vapour-gas channel with simultaneous increase of the stability of its existence and introduction of cathode breaking of the oxide film.

KEYWORDS: aluminium alloys of 7xxx series, laser welding, weld formation, graininess, defects, ways to eliminate

INTRODUCTION

Alloys of 7xxx series (Al–Zn–Mg–Cu system) have the highest strength among aluminium alloys. After heat treatment this value is more than 500 MPa [1]. Owing to a combination of high strength with low density, they are quite attractive for application in manufacture of modern transportation systems [2]. However, the weldability of such alloys is poor, because of the high susceptibility to hot cracking, high coefficient of thermal expansion and low temperature of evaporation of some alloying elements, in particular Zn and Mg [3]. The above drawbacks promote formation of some welding defects, such as cracks and pores, particularly, in the case of laser welding with incomplete (or partial) penetration [4].

Incomplete penetration welds are used for sealing the flanges or some structures with voids, where electronic equipment is located. The welding operation is here performed as an element of finish mounting, and

in the case of full penetration, there is the danger of complete damage of the interior fittings. Here, laser welding is used to minimize or completely eliminate residual deformations. Such structures are used, in particular, in rocket engineering. Their welded joints should ensure tightness and certain strength, but because of relatively short life, the question of cyclic load resistance is not considered. Therefore, consideration of the features of formation of welded joints of aluminium alloys of 7xxx series, in particular, with incomplete penetration, is urgent.

In modern industry, laser welding is ever wider applied. It is used not only in the aerospace industry, but also in car building, in automotive industry and in many other areas of activity [5]. However, this process is still being studied, and it is applied predominantly to produce nondetachable structures from aluminium alloys of 2xxx, 5xxx and 6xxx series [6]. The question of the features of laser welding application to produce a nondetachable structure from 7xxx series alloys has already been considered to some extent in works [6,

Table 1. Element content (wt.%) in high-strength 7005 and 7075 aluminium alloys

Alloy	Definition type	Al	Si	Fe	Cu	Mn
7005	Alloy grader	Base	Up to 0.35	Up to 0.40	Up to 0.10	0.2–0.7
	General analysis	93.12–93.37	0.43–0.72	–	0.18–0.19	0.25–0.33
	Analysis in the grain volume	88.93–92.78	0.51–0.69	–	0.16	0.62–0.64
	Inclusions in the grain volume	–	0.86–1.60	10.81–28.74	0.2–0.3	2.41–3.09
7075	Alloy grader	Base	Up to 0.40	Up to 0.50	1.2–2.0	Up to 0.30
	General analysis	89.84–90.66	0.45–0.62	–	1.53–1.86	0.13–0.27
	Analysis in the grain volume	89.97–90.41	0.55–0.56	–	1.46–1.63	0.12–0.23
	Inclusions in the grain volume	–	0.32–39.51	6.75–29.86	0.94–7.18	0.08–2.83

Table 1 (cont.)

Alloy	Definition type	Mg	Cr	Zn	Ti	Other
7005	Alloy grader	1.0–1.8	0.06–0.20	4–5	0.01–0.06	Zr 0.08–0.20 Other up to 0.15
	General analysis	0.56–0.75	–	5.01–5.37	–	–
	Analysis in the grain volume	0.76–0.80	–	5.1–8.89	–	–
	Inclusions in the grain volume	0.24–0.54	–	2.02–3.57	–	–
7075	Alloy grader	2.1–2.9	0.18–0.28	5.1–6.1	Up to 0.20	Up to 0.15
	General analysis	0.91–1.10	–	6.02–6.45	–	–
	Analysis in the grain volume	1.04–1.12	–	6.41–6.74	–	–
	Inclusions in the grain volume	0.17–30.64	5.32–6.23	1.03–6.91	–	–

7]. So, the basic physical processes of laser radiation interaction with aluminium alloys were considered in work [6], and in work [7] laser welding of 7075 alloy was compared with microplasma and laser-microplasma. It was determined that in laser welding there is the risk of formation of inner pores and hot cracks, in particular those associated with internal inclusions and weld defects.

In work [8] the influence of heat input in laser welding of 7075 alloy on the change of element concentration in the weld and, consequently, on their hot cracking susceptibility was considered. It is rational to consider investigations in this direction, in particular, for the case of making welds with incomplete penetration of the butt. Available research results do not completely disclose a range of important issues, concerning formation of particular structures at application of certain parameters of laser welding mode, formation of characteristic defects (primarily pores and cracks), and determination of the ways to eliminate them.

The objective of this work is formation of characteristic structures of the joints and the risk of appearance of defects of the type of pores and cracks at laser welding of aluminium alloys of 7xxx series, made with partial (nonthrough thickness) penetration.

The following problems were solved to achieve this goal:

- performance of laser welding of samples of 7xxx series alloys, determination of mode parameters by the criteria of sound formation of the upper bead at fixed penetration depth;

- making sections, studying the structural features of the produced welded joints;

- determination of characteristic defects and possible causes for their formation;

- checking the possibility of elimination of the defined defects by using a hybrid laser-microplasma welding process.

Samples from high-strength 7005 and 7075 alloys were prepared to conduct experiments on determination of laser welding mode parameters. Sample size was $50 \times 50 \times \delta$, where $\delta = 1.5$ and 3.0 mm. During the experiments laser welding of fillet joints was performed, focusing on penetration depth of approximately 0.5 – 0.7 mm. Table 1 gives both the published data on chemical composition of these alloys, and our own. The latter are individual element measurements, made by the method of analytical-scanning microscopy. This method was used to determine both the integral content of individual selected elements of the alloy, and their content in the bulk of individual grains. The size of the latter was as follows: for 7005 alloy $Dg = h \times l = (4-7) \times (20-35) \mu\text{m}$, for 7075 alloy $Dg = h \times l = (5-15) \times (30-70) \mu\text{m}$, where h is the height, and l is the length of the grain (Figure 1). The grain shape coefficient was: for 7005 alloy $l/h = 5$, for 7075 $l/h = 4.5-6.0$. HV microhardness at 100 g load was: for 7075 alloy $624-636$ MPa, and for 7075 alloy it was $1050-1240$ MPa.

Experiments were performed using fiberoptic laser of up to 2000 W power (MFSC-2000W model, Max Photonics Company, PRC), as well as a set of plasma welding equipment, which consisted of CEBORA TIG

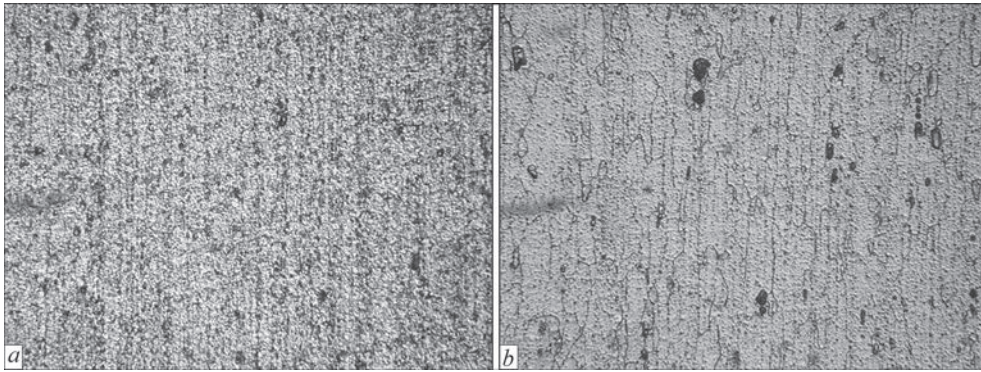


Figure 1. Base metal microstructure ($\times 500$): *a* — 7005 alloy; *b* — 7075



Figure 2. Appearance of a laboratory stand for welding: *a* — laser; *b* — laser- microplasma

AC-DC EVO 450T Robot source and PW30 plasma module (Cebore Company, Italy). A proprietary laboratory stand with replaceable burners was used for laser and laser-microplasma welding (Figure 2). Welding mode parameters were selected by such criteria of sound formation, as absence of caverns and pores, cracks, undercuts on the weld surface that can be recorded visually. The main parameters of the mode are given in Table 2.

To conduct metallographic analysis transverse templates were cut out of the produced joints and microsections were prepared. Here, ion-vacuum etching was used to reveal the microstructure. Results on the made joints were investigated by the methods of optical (Versamet-2 and Neohpot-31 microscopes) and an-

alytical scanning (SEM-515 microscope of PHILIPS Company, Holland) microscopy. Investigations were conducted sequentially in the following sections of the samples: remelted weld metal \rightarrow fusion line \rightarrow HAZ \rightarrow base metal. Optical microscopy was used to study the structural changes in these sections at up to $500\times$ magnifications. Microhardness was measured, using LM-400 microhardness meter (LECO) series). Analytical scanning electron microscopy was used to determine the chemical composition of weld sections (general and local point analysis).

Laser welding by nonthrough thickness welds can be used to produce tight joints, for instance, to weld flanges. Therefore, technological studies were performed by welding simulators in the form of fil-

Table 2. Main welding mode parameters of 7005 and 7075 alloy samples

Welding	Laser radiation power, W	Microplasma power, W		Welding speed V , mm/s	Gas flow rate (Ar), l/min	
		Straight polarity	Reverse polarity		Plasma gas	Shielding gas
Laser	400	–	–	66.7	–	8
Microplasma	–	900	500	5	0.3	18
Laser-microplasma	200	1300	600	66.7	10	30

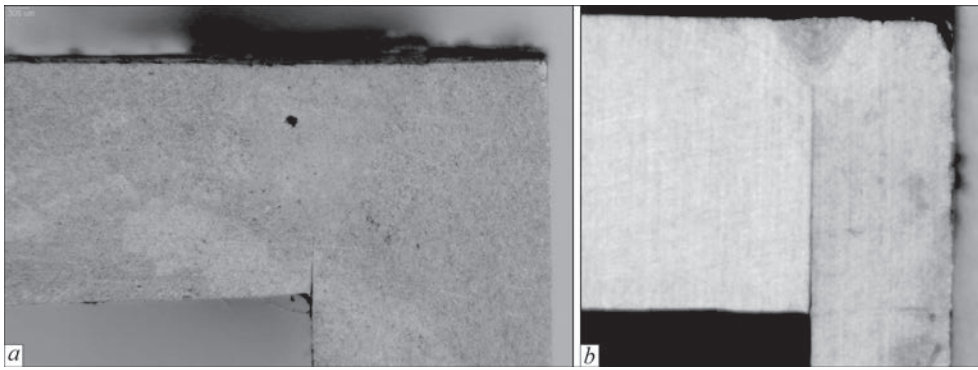


Figure 3. Transverse sections of fillet joints of 7075 alloy, made by laser welding: *a* — at 800 W power and 41.7 ms/s speed; *b* — at 400 W power and 66.7 mm/s speed

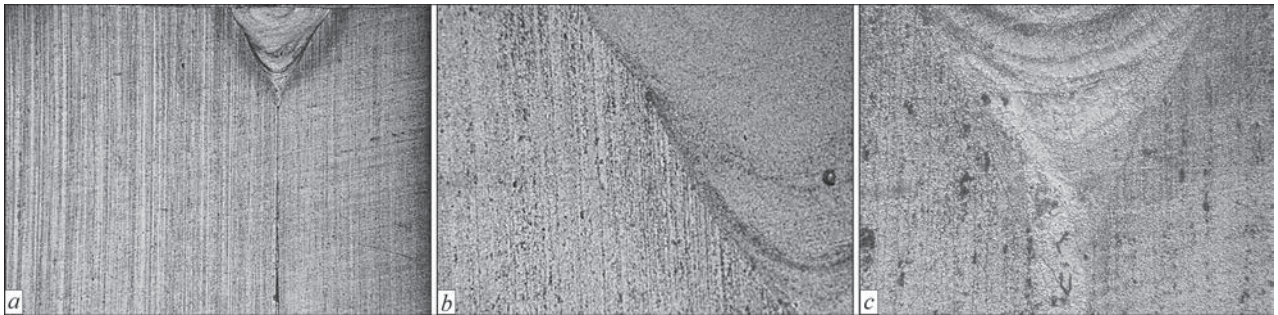


Figure 4. Microstructures of 7005 alloy joints produced by laser welding: *a* — general view of penetration, $\times 50$; *b* — fusion zone; $\times 250$; *c* — stringer precipitates of oxide type in the root zone, $\times 500$

let joints. Preliminary studies on selection of welding mode parameters showed that in order to satisfy the condition of weld formation without caverns (pores), cracks or undercuts on the surface, greater power at lower speed can be used (Figure 3, *a*). This, however, leads to noncompliance with the penetration depth criterion. To meet this criterion, the mode was corrected in combination with the above-mentioned conditions (Figure 3, *b*).

At laser welding of 7005 alloy samples welds of about 0.6 mm (Figure 4, *a*) width and depth were produced. Individual pores of 10–15 μm size were detected in the weld (Figure 4, *b*). The total volume fraction of the defects (V_D) in the weld metal is equal to about 2%. In the center of weld metal the structure consists of grains of an equiaxed shape of size $D_g = 10\text{--}15 \mu\text{m}$. Closer to the fusion line elongated grains of size $D_g = (5\text{--}10)\times(15\text{--}25) \mu\text{m}$ (shape coefficient of 2.5–3.0)

are observed. Metal stringer precipitates of oxide type of size $l_{\text{Al}_2\text{O}_3} = 15\text{--}20 \mu\text{m}$ were detected in the root part of the weld (Figure 4, *c*). The size of the HAZ is of the order of 225 μm . The size of grains in the HAZ is equal to $D_g = (5\text{--}10)\times(15\text{--}50) \mu\text{m}$ (shape coefficient of 3–5). Below the weld in the welded plate material the graininess is equal to $D_g = (4\text{--}5)\times(10\text{--}12) \mu\text{m}$ on the one side and $D_g = (5\text{--}6)\times(15\text{--}20) \mu\text{m}$ on the other side (shape coefficient of 2.5–3).

HV microhardness in the weld center is equal to 613–624 MPa, in the fusion zone it is ~ 602 MPa, in the HAZ it rises up to 631–648 MPa (Figure 5).

Results of chemical element distribution in the joint zones are given in Table 3. It is found that a certain redistribution of elements took place in the weld and HAZ metal within the grain volume and in the overall volume of these zones. No alloying element loss was recorded.

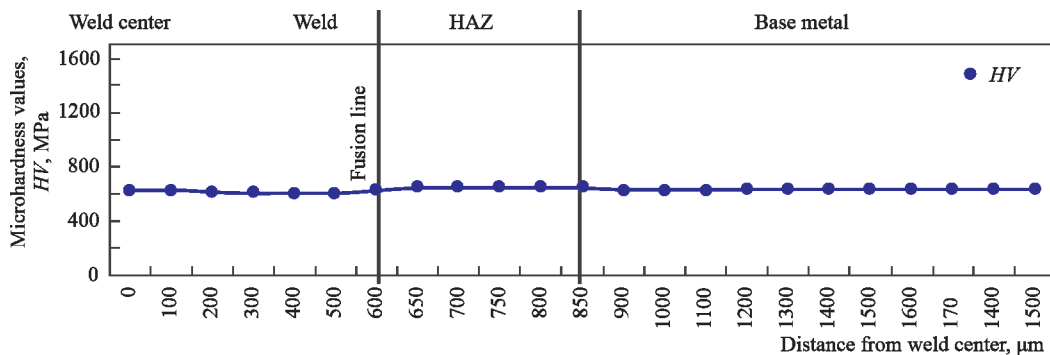


Figure 5. Distribution of HV microhardness (100 g load) from the weld axis towards the base metal in 7005 alloy

Table 3. Results of determination of the content of the main elements by the method of analytical scanning electron microscopy in laser-welded joints of 7005 alloy

Investigation zone	Analysis type	Element content, wt. %					
		Al	Mg	Si	Mn	Cu	Zn
Weld metal	General analysis	92.4–96.22	0.5–0.64	0.13–0.52	0.51–0.88	0.01–0.13	2.4–4.38
	Analysis in the grain volume	91.98–95.91	0.02–0.47	0.4–0.7	0.55–0.87	0.17–0.23	3.02–6.53
HAZ	General analysis	94.0–94.72	0.55–0.74	0.53–0.61	0.41–0.54	0.43	3.55–4.81
	Analysis in the grain volume	93.01–93.17	0.69–0.7	0.45–0.48	0.58–0.63	0.07–0.23	4.85–5.13
Base metal	General analysis	94.66–95.02	0.63–0.66	0.43–0.72	0.27–0.35	0.18–0.29	4.05–4.36
	Analysis in the grain volume	90.41–94.79	0.56–0.92	0.51–0.69	0.49–0.95	0.16	3.38–4.17

Welds approximately 0.64 mm wide and approximately 0.74 mm deep were produced at laser welding of 7075 alloy samples (Figure 6, a). Individual pores of size $d_p = 10\text{--}30\ \mu\text{m}$ were detected in the weld. The overall total volume fraction of defects (V_d) in the weld metal is close to 3 %. The structure in the weld metal center is characterized by equiaxed grains of size $D_g = 15\text{--}25\ \mu\text{m}$. Closer to the fusion line in the weld metal elongated grains of size $D_g = (5\text{--}10) \times (20\text{--}50)\ \mu\text{m}$ (shape coefficient of 2–5) are observed. In the root part of the weld metal, stringer precipitates of oxide type of size $l_{\text{Al}_2\text{O}_3} = 5\text{--}15\ \mu\text{m}$ were detected, the arrangement of which follow the shape of the root part (Figure 6, c). The width of the HAZ in this joint is equal to 200–240 μm (Figure 6, a). Grain size in the HAZ is $D_g = (10\text{--}15) \times (30\text{--}50)\ \mu\text{m}$ (shape coefficient of 3–3.5). Below the weld in the welded plate material, the graininess is equal to $D_g = (10\text{--}25) \times (45\text{--}50)\ \mu\text{m}$ (shape coefficient of 3–3.5). Below the weld in the welded plate material the grain-

iness is $D_g = (10\text{--}25) \times (45\text{--}50)\ \mu\text{m}$ on the one side and $D_g = (5\text{--}25) \times (20\text{--}75)\ \mu\text{m}$ on the other.

HV microhardness of the weld metal is equal to 958–980 MPa, in the fusion zone it is 829–936 MPa, in the HAZ it rises on average by 20 % relative to the weld metal and is equal to 1030–1070 MPa (Figure 7).

Results of chemical element distribution in the joint zones are given in Table 4. It was established that a certain redistribution of elements in the grain volume and in the overall volume of these zones occurred in the weld and HAZ metal. No alloying element loss was recorded.

In case of welding 7005 alloy, liquid metal flowing into the slot of the butt being welded is observed in the root part of the weld (Figure 4, a). It is attributable to the high fluidity of this alloy, as well as the known effect of formation of spiked structure in the root zone (see, for instance, work [9]). Presence of fine pores in the root part of the weld (Figure 6, b) in the case



Figure 6. Microstructure of 7075 alloy joints produced by laser welding: a — general view of penetration, $\times 20$; b — pores in the root zone, $\times 250$; c — stringer precipitates of oxide type in the root zone, $\times 500$

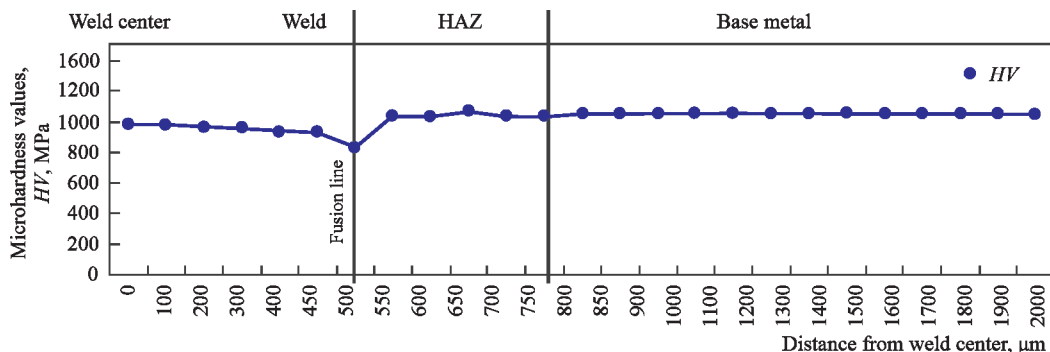


Figure 7. HV microhardness distribution (100 g load) from weld axis towards base metal in the joint of 7075 alloy

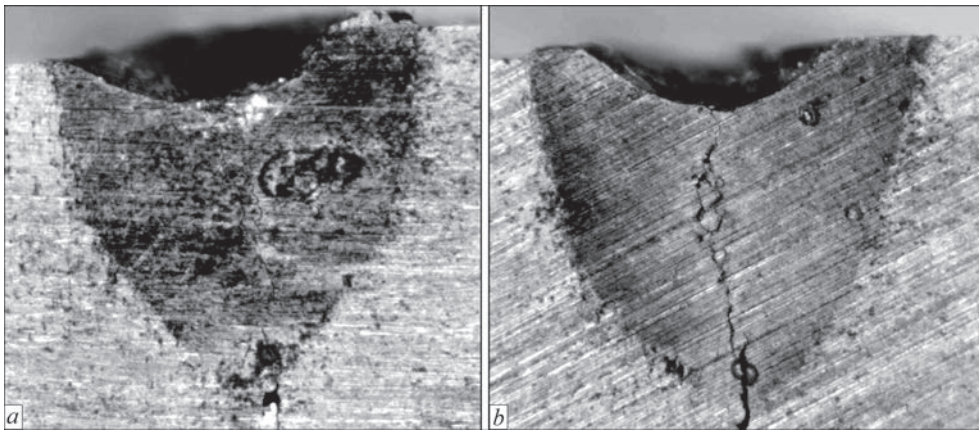


Figure 8. Transverse sections of laser-welded joints of 7075 alloy: *a* — $E \approx 25$ J/mm; *b* — 35

Table 4. Results of determination of the main element content by the method of scanning electron microscopy in laser-welded joint of 7075 alloy

Examined zone	Analysis type	Element content, wt.%					
		Al	Mg	Si	Mn	Cu	Zn
Weld metal	General analysis	89.79–90.17	1.04–1.11	0.47–0.49	0.08–0.14	1.83–2.02	6.05–6.61
	Analysis in the grain volume	89.33–90.27	0.97–1.01	0.42–0.65	0.12–0.17	1.74–2.04	6.17–7.11
HAZ	General analysis	88.79–89.91	1.05–1.16	0.27	0.12	1.2–2.29	6.78–7.38
	Analysis in the grain volume	89.53–89.54	1.13–1.24	0.5–0.71	0.05–0.16	1.72–1.84	6.73–6.84
Base metal	General analysis	89.84–90.66	0.91–1.1	0.45–0.62	0.13–0.27	1.53–1.86	6.02–6.45
	Analysis in the grain volume	89.84–90.41	1.04–1.12	0.55–0.56	0.12–0.17	1.46–1.63	6.41–6.74

of welding 7075 alloy is explained by penetration of air from the butt. Stringer precipitates of oxide film, which are observed in welding both the alloys, are attributable to penetration of fragments of this film into the weld pool, which were left or formed on the edges being welded.

Absence of hot cracks in the samples analyzed above, is attributable to the selected high-speed welding mode, where the heat input was equal to the order of $E = 5$ J/mm (Figure 3, *b*). In case of increase of the heat input up to values $E = 5$ –30 J/mm the cracking susceptibility becomes higher. In this value range, variants of producing welds without cracks, for instance at $E \approx 20$ J/mm (Figure 3, *a*), or with crack initiation in the weld root at $E \approx 25$ J/mm (Figure 8, *a*). At heat input above ~ 30 J/mm in case of welding 7075 alloy, there is the risk of hot crack formation (Figure 8, *b*). Such cracks initiate in the weld root zone, also on root defects of pore type, and can extend for its entire height.

In order to remove the defects in the weld root part, it is rational to reduce and stabilize the vapour-gas channel pulsations, which lead to formation of the spike structure. In order to eliminate the risk of formation of stringer precipitates of oxide film, it is rational to break it up in the weld pool, for instance, using an electric arc of reverse polarity. It is known from work [10] that hybrid laser-arc processes promote stabili-

zation of the spike structure of the weld root, and the cathodic cleaning effect at application of laser-plasma welding is known from work [11]. The laboratory stand, shown in Figure 2, *b*, was used to conduct preliminary studies on laser-microplasma welding of 7005 and 7075 alloys. No presence of stringer precipitates of oxide type (oxide film inclusions) in the remelted metal was revealed here. The proneness to porosity in the weld root part decreased. Thus, replacement of laser welding by hybrid laser-microplasma process can be regarded as one of the rather effective ways to eliminate the detected characteristic defects.

CONCLUSIONS

1. It was established that when producing welded joints of aluminium alloys of 7xxx series of 1.5 mm thick sheets by fiber laser welding with partial (nonthrough thickness) penetration to the depth of 0.5–0.7 mm, there is the risk of formation of pores, in particular, in the root zone, stringer precipitates of oxide film in the weld lower part, as well as hot cracks. Elimination of the latter is possible due to decrease of welding heat input below 25–30 J/mm.

2. Weld metal is characterized by an equiaxed fine structure with grain size of 10–15 μm for 7005 alloy and 15–25 μm for 7075 alloy. In the fusion zone the grains have an elongated shape with the coefficient from 2.5 to 3 for 7005 alloy and 2–5 for 7075 alloy. In

the HAZ the grain length is reduced, shape coefficient becomes 3–5 and 3.0–3.5 for 7005 and 7075 alloys, respectively.

3. During performance of laser welding with small (~5 J/mm) values of heat input the microhardness of the welds and HAZ become rather uniform, and close to that of base metal microhardness. For 7075 alloy in the region of the fusion zone a reduction of microhardness to 20 % was observed, which is due to formation of grains of an elongated shape with shape coefficient of 2–5.

4. Elimination of the found drawbacks can be achieved by reducing the vapour-gas channel pulsations with simultaneous improvement of the stability of its existence and introduction of cathode breaking of oxide film.

The work was performed with the support of the following projects:

1. *The National Key Research and Development Program of China — in the framework of the strategy «One Belt — One Road» (grant number 2020YFE0205300);*

2. *Strategic project of the Academy of Sciences of Guangdong Province, (GDAS'Project of Science and Technology Development, 2020GDASYL-20200301001), China;*

3. *Project of the Guangzhou Economic and Technological Development Zone 2019GH19, China.*

REFERENCES

1. Varshney, D., Kumar, K. (2021) Application and use of different aluminium alloys with respect to workability, strength and welding parameter optimization. *Ain Shams Engineering J.*, 12(1), 1143–1152. DOI: <https://doi.org/10.1016/j.asej.2020.05.013>
2. Kang, M., Kim, C. (2017) A review of joining processes for high strength 7xxx series aluminum alloys. *J. of Welding and Joining*, 35(6), 79–88. DOI: <https://doi.org/10.5781/JWJ.2017.35.6.12>
3. Löveborn, D., Larsson, J. K., Persson, K.-A. (2017) Weldability of aluminium alloys for automotive applications. *Physics Procedia*, 89, 89–99. DOI: <https://doi.org/10.1016/j.phpro.2017.08.011>
4. Kang, M., Cheon, J., Kam, D.-H., Kim, C. (2021) The hot cracking susceptibility subjected the laser beam oscillation welding on 6XXX aluminum alloy with a partial penetration joint. *J. of Laser Applications*, 33, 012032. DOI: <https://doi.org/10.2351/7.0000319>
5. Kim, C.-H., Ahn, Y.-N., Lim, H.-S. (2011) Laser welding of automotive aluminum alloys. *J. of Welding and J.*, 29(4), 21–26. DOI: <https://doi.org/10.5781/KWJS.2011.29.4.383>
6. Zhao, H., White, D.R., DebRoy, T. (1999) Current issues and problems in laser welding of automotive aluminium alloys. *International Materials Reviews*, 44(6), 238–266. DOI: <https://doi.org/10.1179/095066099101528298>
7. Korzhyk, V., Khaskin, V., Grynyuk, A. et al. (2022) Comparison of the features of the formation of joints of aluminium alloy 7075 (Al–Zn–Mg–Cu) by laser, microplasma, and laser-microplasma welding. *Eastern-European J. of Enterprise Technologies*, 115(1/12), 38–47. DOI: <https://doi.org/10.15587/1729-4061.2022.253378>
8. Holzer, M., Hofmann, K., Mann, V. et al. (2016) Change of hot cracking susceptibility in welding of high strength aluminium alloy AA 7075. *Physics Procedia*, 83, 463–471. DOI: <https://doi.org/10.1016/j.phpro.2016.08.048>
9. Fetzer, F. (2018) Fundamental investigations on the spiking mechanism by means of laser beam welding of ice. *J. of Laser Applications*, 30(1), 012009-1–012009-9. DOI: <https://doi.org/10.2351/1.4986641>
10. Shelyagin, V.D., Khaskin, V.Yu., Garashchuk, V.P. et al. (2002) Hybrid CO₂-laser and CO₂ consumable-arc welding. *The Paton Welding J.*, 10, 35–38.
11. Krivtsov, I.V., Shelyagin, V.D., Khaskin, V.Yu. et al. (2007) Hybrid laser-plasma welding of aluminium alloys. *The Paton Welding J.*, 5, 36–40.

ORCID

V.M. Korzhyk: 0000-0001-9106-8593,
 V.Yu. Khaskin: 0000-0003-3072-6761,
 A.A. Grynyuk: 0000-0002-6088-7980,
 S.I. Peleshenko: 0000-0001-6828-2110,
 Yao Yuhui: 0000-0001-7196-1317,
 S.G. Hrygorenko: 0000-0003-0625-7010,
 V.O. Shcheretskyi: 0000-0002-8561-4444,
 O.S. Kushnareva: 0000-0002-2125-1795

CONFLICT OF INTEREST

The Authors declare no conflict of interest

CORRESPONDING AUTHOR

V.M. Korzhyk
 E.O. Paton Electric Welding Institute of the NASU
 11 Kazymyr Malevych Str., 03150, Kyiv, Ukraine
 E-mail: vnkorzhyk@gmail.com

SUGGESTED CITATION

V.M. Korzhyk, V.Yu. Khaskin, A.A. Grynyuk, S.I. Peleshenko, Yao Yuhui, S.G. Hrygorenko, V.O. Shcheretskyi, O.S. Kushnareva (2022) Fibre laser welding of aluminium alloys of 7xxx series (Al–Zn–Mg–Cu) by nonthrough thickness welds. *The Paton Welding J.*, 4, 19–25.

JOURNAL HOME PAGE

<https://pwj.com.ua/en>

Received: 28.03.2022

Accepted: 30.06.2022